Supplementary information

Bimetallic phosphide $Ni_xCo_{1-x}P$ decorated flower-like $ZnIn_2S_4$ for enhanced photocatalytic hydrogen evolution

Yumeng Wang, Tingting Zhang, Tingting Wei, Fengyan Li*, Lin Xu*

Key Laboratory of Polyoxometalate and Reticular Material Chemistry of Ministry of Education, College of Chemistry, Northeast Normal University, Changchun 130024, P. R. China.

Materials

All reagents were of analytical grade without further purification, including Zinc chloride($ZnCl_2$), Indi um(III) chloride tetrahydrate($InCl_3 \cdot 4H_2O$, 99%), thioacetamide (CH_3CSNH_2, TAA), Cobalt nitrate hexah ydrate ($Co(NO_3)_2 \cdot 6H_2O$)from Aladdin, Glycerol, hydrochloric acid (HCl, 36%),sodium hypophosphite m onohydrate ($NaH_2PO_2 \cdot 2H_2O$, ≥98.0%), nickel nitrate hexahydrate ($Ni(NO_3)_2 \cdot 6H_2O$) were achieved throu gh Sinopharm Chemical Reagent Co., Ltd. Deionized (DI) water was used during the whole experime nt process.

Characterization

The obtained products were characterized by X-ray diffraction(XRD, RigakuSmartlab SE, Japan) and XRD patterns were obtained at 10°–80° at a scanning rate of 10° min^{-1}. A scanning electron microscope (Hitachi SU-8000 FE-SEM) was used to characterize the morphology and size of the powder samples. Transmission electron microscopy (TEM, JEM 2100-F) operated at an accelerating voltage of 200 kV. The X-ray photoelectron spectroscopy was used to analyze the chemical states of the synthetic products using a USWHA150 photoelectron spectrometer with a monochromatic Al Kα excitation source, and the binding energies of all elements are calibrated by C 1s at 284.8 eV. Ultraviolet–visible diffuse reflectance spectra (DRS) was measured with a UV-vis spectrophotometer (Varian Cary 500) in the range 200–800 nm. Photoluminescence (PL) ments were carried out on an F-7000 fluorescence spectrophotometer at room temperature.

Photoelectrochemical testing

The Nyquist plots, photocurrent measurements and Mott-Schottky (MS) Measurements were all recorded by a CHI660E electrochemical workstation (Shanghai Chenhua Instrument Co. Ltd.) in a 0.5 M aqueous Na_2SO_4 solution electrolyte, using astandard three-electrode system, where an saturated calomel electrode (SCE) and a platinum wire electrode were used as the reference and counter electrodes, respectively. The working electrode utilized samples wrapped F-doped tin oxide (FTO) glasses.

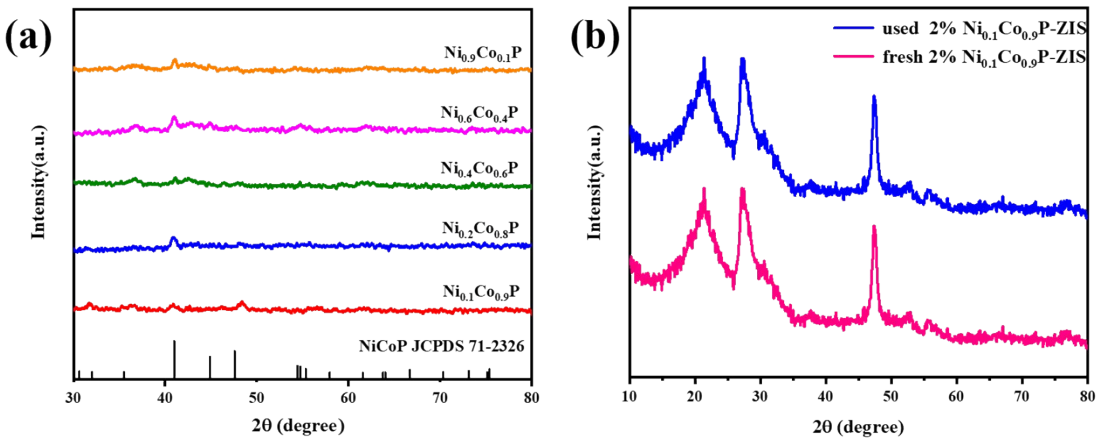

Fig. S1 XRD patterns of (a) $Ni_xCo_{1-x}P$ (b) the fresh and used $Ni_{0.1}Co_{0.9}P$-ZIS.

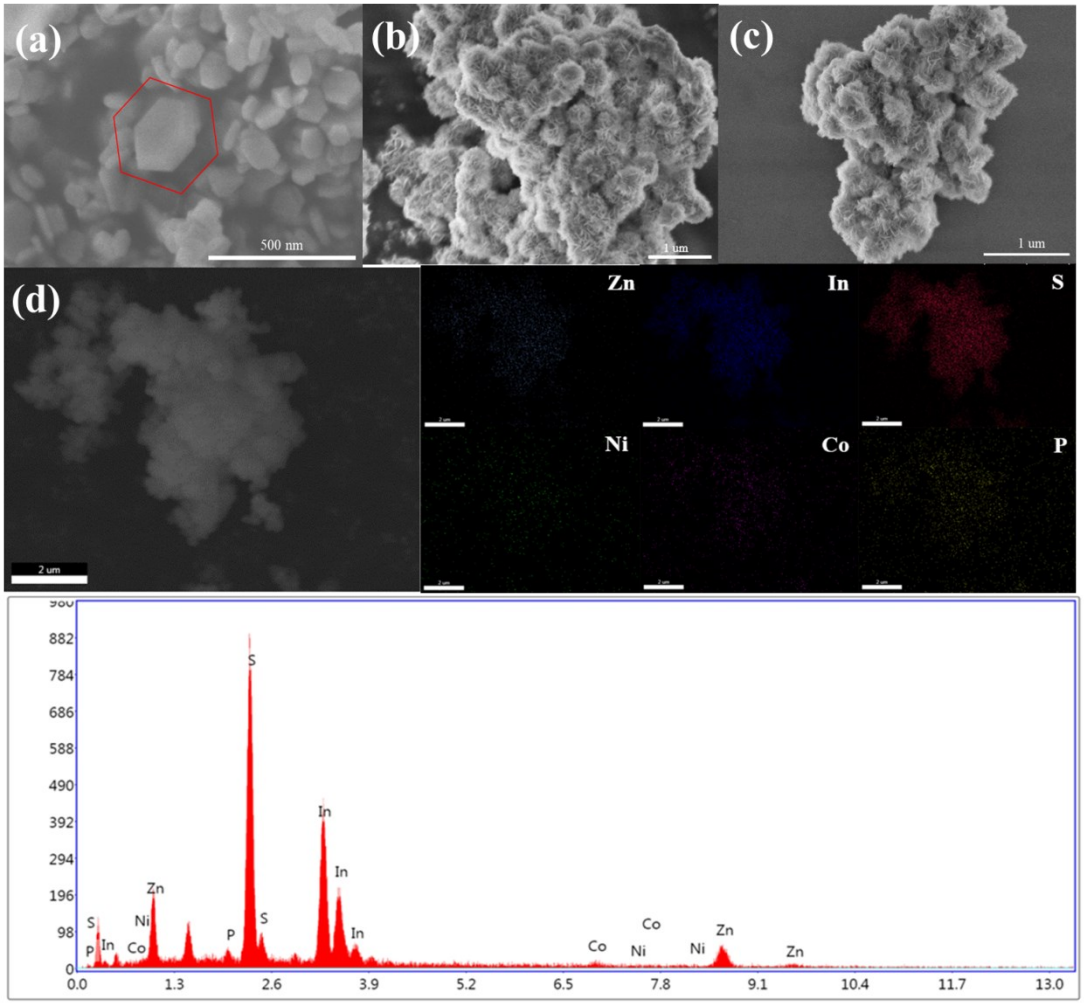

Fig. S2 SEM image of $Ni_{0.1}Co_{0.9}P$(a), fresh 2%$Ni_{0.1}Co_{0.9}P$-ZIS(b), used 2%$Ni_{0.1}Co_{0.9}P$-ZIS (c), HAADF-STEM of 2%$Ni_{0.1}Co_{0.9}P$-ZIS(d), Energy-dispersive X-ray (EDX) spectrum of 2%$Ni_{0.1}Co_{0.9}P$-ZIS(e).

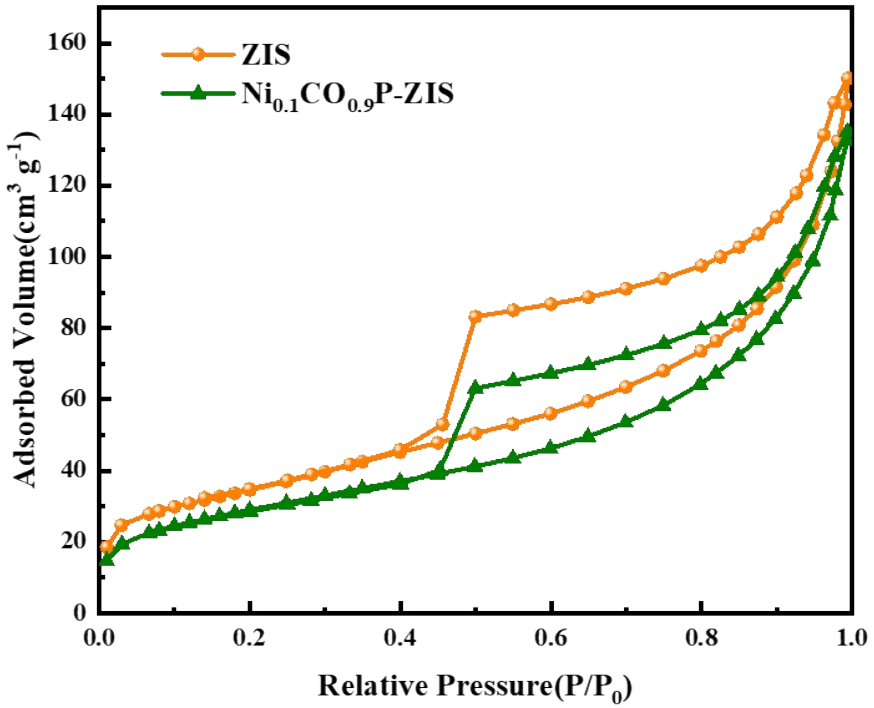

Fig. S3 Nitrogen adsorption-desorption isotherms of pure ZIS and $Ni_{0.1}Co_{0.9}P$-ZIS.

Table S1 Summary of BET, pore volume of as-prepared pure ZIS and $Ni_{0.1}Co_{0.9}P$-ZIS.

	$S_{BET}(m^2/g)$	Pore volume(cm^3/g)
Pure ZIS	123.8	0.19
2%$Ni_{0.1}Co_{0.9}P$-ZIS	105.5	0.17

Table S2 The specific charge transfer resistance(R_{ct}) of ZIS, Ni_2P-ZIS, CoP-ZIS, $Ni_{0.1}Co_{0.9}P$-ZIS.

Photocatalyst	R_{ct}(kΩ)
$ZnIn_2S_4$	**57.57**
Ni_2P-$ZnIn_2S_4$	**52.87**
CoP-$ZnIn_2S_4$	**47.44**
$Ni_{0.1}Co_{0.9}P$- $ZnIn_2S_4$	**18.12**

Table S3 The performance comparison of different $ZnIn_2S_4$ based Photocatalyst

Photocatalyst	Photocatailstic H_2 evolution Rate	Weight	Cocatalyst	Sacrificial agent	Reference
$Ni_{0.1}Co_{0.9}P$/ZIS	3839 μmol $g^{-1}\cdot h^{-1}$	300 W Xe (>420 nm)	/	TEOA	This work
Cu_3P/ZIS	2091.1 $umol\cdot h^{-1}\cdot g^{-1}$	300 W Xe (>420 nm)	/	Na_2S/Na_2SO_3	[1]
Ni_2P/ ZIS	2066 $umol\cdot h^{-1}\cdot g^{-1}$	300 W Xe (>420 nm)	/	lactic acid	[2]
$Ni_{12}P_5$/ZIS	2263 $umol\cdot h^{-1}\cdot g^{-1}$	300 W Xe (>420 nm)	/	Na_2S/Na_2SO_3	[3]
$CoFe_2O_4$/ZIS	800 $umol\cdot h^{-1}\cdot g^{-1}$	300 W Xe (>420 nm)	Pt	TEOA	[4]
WO_3/ ZIS	2202.9 $umol\cdot h^{-1}\cdot g^{-1}$	300 W Xe (>420 nm)	/	Na_2S/Na_2SO_3	[5]
CeO_2/ZIS	847.42 $umol\cdot h^{-1}\cdot g^{-1}$	300 W Xe (>420 nm)	/	Na_2S/Na_2SO_3	[6]
BP/$ZnIn_2S_4$	1278 $umol\cdot h^{-1}\cdot g^{-1}$	300 W Xe (>420 nm)	Pt	Na_2S/Na_2SO_3	[7]
2D/2D ZIS/MoS_2	4974 $umol\cdot h^{-1}\cdot g^{-1}$	300 W Xe (>400 nm)	/	lactic acid	[8]
2D/2D g-C_3N_4/ZIS	2780 $umol\cdot h^{-1}\cdot g^{-1}$	300 W Xe (>420 nm)	/	TEOA	[9]
$CuInS_2$/ZIS	1168 $umol\cdot h^{-1}\cdot g^{-1}$	300 W Xe (>420 nm)	/	Na_2S/ Na_2SO_3	[10]
$In(OH)_3$/ZIS	2088 $umol\cdot h^{-1}\cdot g^{-1}$	300 W Xe (>420 nm)	/	Na_2S/ Na_2SO_3	[11]
CdS/QDs/ZIS	2107.5 $umol\cdot h^{-1}\cdot g^{-1}$	300 W Xe (>420 nm)	/	lactic acid	[12]
ZnS/ZIS	453.4 $umol\cdot h^{-1}\cdot g^{-1}$	300 W Xe (AM 1.5)	/	TEOA	[13]
WS_2/ZIS	199.1 $umol\cdot h^{-1}\cdot g^{-1}$	300 W Xe (>420 nm)	/	Na_2S/ Na_2SO_3	[14]
AgO_2/ ZIS	2334.1 $umol\cdot h^{-1}\cdot g^{-1}$	300 W Xe (>420 nm)	Pt	TEOA	[15]

Reference

1 Z. Yang, L. Shao, L. Wang, X. Xia, Y. Liu, S. Cheng, C. Yang and S. Li, Boosted photogenerated carriers separation in Z-scheme $Cu_3P/ZnIn_2S_4$ heterojunction photocatalyst for highly efficient H_2 evolution under visible light, *Int. J. Hydrogen Energy*, 2020, **45**, 14334-14346.

2 X. L. Li, X. J. Wang, J. Y. Zhu, Y. P. Li, J. Zhao and F.T. Li, Fabrication of two-dimensional $Ni_2P/ZnIn_2S_4$ heterostructures for enhanced photocatalytic hydrogen evolution, *Chem. Eng. J.*, 2018, **353**, 15-24.

3 D. Zeng, Z. Lu, X. Gao, B. Wu and W. J. Ong, Hierarchical flower-like $ZnIn_2S_4$ anchored with well-dispersed $Ni_{12}P_5$ nanoparticles for high-quantum-yield photocatalytic H_2 evolution under visible light, *Catal. Sci. Technol.*, 2019, **9**, 4010-4016.

4 C. Li, H. Che, P. Huo, Y. Yan, C. Liu and H. Dong, Confinement of ultrasmall $CoFe_2O_4$ nanoparticles in hierarchical $ZnIn_2S_4$ microspheres with enhanced interfacial charge separation for photocatalytic H_2 evolution, *J. Colloid Interface Sci.*, 2020, **581**, 764-773.

5 L. Ye and Z. Wen, ZnIn2S4 nanosheets decorating WO_3 nanorods core-shell hybrids for boosting visible-light photocatalysis hydrogen generation, *Int. J. Hydrogen Energy*, 2019, **44**, 3751-3759.

6 M. Zhang, J. Yao, M. Arif, B. Qiu, H. Yin, X. Liu and S.-m. Chen, 0D/2D $CeO_2/ZnIn_2S_4$ Z-scheme heterojunction for visible-light-driven photocatalytic H_2 evolution, *Appl. Surf. Sci.*, 2020, **526**, 145749.

7 Q. Zhang, J. Zhang, L. Zhang, M. Cao, F. Yang and W.-L. Dai, Facile construction of flower-like black phosphorus nanosheet@ $ZnIn_2S_4$ composite with highly efficient catalytic performance in hydrogen production, *Appl. Surf. Sci.*, 2020, **504**, 144366.

8 L. Huang, B. Han, X. Huang, S. Liang, Z. Deng, W. Chen, M. Peng and H. Deng, Ultrathin 2D/2D $ZnIn_2S_4/MoS_2$ hybrids for boosted photocatalytic hydrogen evolution under visible light, *J. Alloys Compd.*, 2019, **798**, 553-559.

9 B. Lin, H. Li, H. An, W. Hao, J. Wei, Y. Dai, C. Ma and G. Yang, Preparation of 2D/2D g-C_3N_4 nanosheet@ $ZnIn_2S_4$ nanoleaf heterojunctions with well-designed high-speed charge transfer nanochannels towards high-efficiency photocatalytic hydrogen evolution, *Appl., Catal. B,* 2018, **220**, 542-552.

10 X. Guo, Y. Peng, G. Liu, G. Xie, Y. Guo, Y. Zhang and J. Yu, An Efficient ZnIn2S4@ CuInS2 Core–Shell p–n Heterojunction to Boost Visible-Light Photocatalytic Hydrogen Evolution, *J. Phys. Chem. C*, 2020, **124**, 5934-5943.

11 H. Zhao, T. Zhang, D. Shan, Y. Zhu, G. Gao, Y. Liu, J. Liu, M. Liu and W. You, $ZnIn_2S_4/In(OH)_3$ hollow microspheres fabricated by one-step l-cysteine-mediated hydrothermal growth for enhanced hydrogen production and MB degradation, *Int. J. Hydrogen Energy*, 2020, **45**, 13975-13984.

12 W. Chen, R.-Q. Yan, J.-Q. Zhu, G.-B. Huang and Z. Chen, Highly efficient visible-light-driven photocatalytic hydrogen evolution by all-solid-state Z-scheme $CdS/QDs/ZnIn_2S_4$ architectures with MoS_2 quantum dots as solid-state electron mediator, *Appl. Surf. Sci.*, 2020, **504**, 144406.

13 H. Song, N. Wang, H. Meng, Y. Han, J. Wu, J. Xu, Y. Xu, X. Zhang and T. Sun, A facile synthesis of a ZIF-derived $ZnS/ZnIn_2S_4$ heterojunction and enhanced photocatalytic hydrogen evolution, *Dalton Trans.*, 2020, **49**, 10816-10823.

14 J. Zhou, D. Chen, L. Bai, L. Qin, X. Sun and Y. Huang, Decoration of WS_2 as an effective noble-metal free cocatalyst on $ZnIn_2S_4$ for enhanced visible light photocatalytic hydrogen evolution, *Int. J. Hydrogen Energy*, 2018, **43**, 18261-18269.

15 Y. Xiao, Z. Peng, W. Zhang, Y. Jiang and L. Ni, Self-assembly of Ag2O quantum dots on the surface of $ZnIn_2S_4$

nanosheets to fabricate pn heterojunctions with wonderful bifunctional photocatalytic performance, *Appl. Surf. Sci.*, 2019, **494**, 519-531.